International Forum on Aeroelasticity and Structural Dynamics
IFASD 2019
9-13 June 2019, Savannah, Georgia, USA

FLUTTER ANALYSIS OF CURVED WINGS USING FULLY INTRINSIC EQUATIONS

M.R. Amoozgar[1], S.A. Fazelzadeh[2], H. Haddad Khodaparast[1], M.I. Friswell[1], and J.E. Cooper[3]

[1] College of Engineering, Swansea University
Swansea, Wales SA2 8PP, United Kingdom
m.amoozgar@swansea.ac.uk
h.haddadkhodaparast@swansea.ac.uk

[2] School of Mechanical Engineering, Shiraz University
Shiraz, 71963-16548, Iran
fazelzad@shirazu.ac.ir

[3] Department of Aerospace Engineering, University of Bristol
Bristol, BS8 1TR, United Kingdom
j.e.cooper@bristol.ac.uk

Keywords: Aeroelastic stability, curved wing, fully intrinsic equations, veering, unsteady aerodynamics.

Abstract: In this paper, the aeroelastic instability of a curved wing is investigated. The wing structure is modeled by using the geometrically exact fully intrinsic beam equations, and the aerodynamic loads are simulated through the incompressible unsteady aerodynamic model. The wing is considered to have initial out of plane curvature, and the effect of the curvature on the flutter speed and frequency of the wing is determined. Two curved wing case studies are considered here. In the first case, the span of the wing is assumed to be constant and therefore as the wing is curved the projected area of the wing decrease. In the second case, the wing is assumed to have a constant projected area and therefore different curvature angles result in different span lengths. When the initial curvature is added to the wing, the dynamics of the wing changes, and therefore the aeroelastic stability of the wing is also affected. It is shown that when the initial curvature of the wing increases, at first the flutter speed decreases and then increases and finally a sudden jump occurs in the flutter speed due to the change of coupled modes contributing in flutter. Moreover, the flutter frequency also first decreases by increasing the curvature of the wing, and then there is a sudden jump in the frequency, and from this point again the frequency decreases. Finally, results highlighting the importance of the initial curvature of the wing on the flutter speed and frequency of these two case studies are presented.

1 INTRODUCTION

The aeroelasticity of aircraft wings is a topic of interest especially for flexible aircraft. In this case, the mutual interaction of structural dynamics and aerodynamic loads may result in

limitations in the operational condition of the aircraft. For a safe airplane, the flutter instability should stay well beyond the flight envelope, and therefore it is very important to find the flutter instability envelope of the aircraft. Flutter analysis of aircraft wings has been an active research topic since 1917. One of the first studies that dealt with the flutter analysis was presented by Bairstow and Fage [1]. They studied the reason for the flutter instability that occurred in the horizontal tail of the twin-engined Handly Page O/400. Goland [2] studied the flutter of a uniform aircraft wing by integrating the differential equations. Then, the effect of adding wing-tip weights on the flutter of the wing was studied by Goland and Luke [3]. The shape of the wing planform is one of the important factors that derives the performance characteristics of aircraft. Usually, the planform shape of the wing is a tradeoff between different flight conditions and is not always the optimized shape for each flight condition. Therefore, the idea of changing the planform of the wing in flight to obtain the optimized shape of the wing in each flight condition has been proposed [4, 5]. Morphing wings enhance the performance of the wing by changing the shape in flight by using a proper mechanism [4, 5]. However, when the planform of the wing changes, the aeroelastic stability of the wing is also affected. Therefore, the aeroelastic stability of such wings should also be considered.

Changing the sweep of the wing in flight was one of the earliest ways of changing planform in flight to reach higher cruise speeds. Lottati [6] showed the importance of the sweep angle on the aeroelastic stability of a composite wing. Gern and Librescu [7] studied the effect of external masses mounted under the wing on the aeroelastic stability of swept wings. The aeroelastic instability of a swept wing under the effect of an engine was considered by Mazadi and Fazelzadeh [8]. They showed that the combination of sweep angle of the wing, and the engine mass and thrust, influenced the flutter speed and frequency of the wing. Adding winglets to the tips of wings is another way of altering the aerodynamic loads which can result in lower loads on the wing. When a winglet is added to the wing, the aeroelastic properties of the clean wing changes. Goetz et al. [9] showed numerically and experimentally that when tip fins are introduced to the wing, the flutter speed changes, and this is due more to the structural effects. Moreover, the effect of winglet stiffness and mass on the aeroelastic stability of wings was studied by Dogget and Farmer [10]. They showed that when the winglet is added to the wing, the flutter dynamic pressure reduces, and for heavier winglets a larger reduction was observed. Peng and Jinglong [11] considered the aeroelasticity of wings with C-type wing tips. They concluded that when the winglet is added to transport aircraft wings the flutter speed reduces by about 10%. More recently, the effect of winglets on the transonic aeroelasticity of a transport aircraft wing was studied experimentally by Lv et al. [12]. They showed that the winglet shape doesn't affect the flutter speed significantly, while the weight of the winglet significantly reduces the flutter speed. They also highlighted that the aerodynamics of the winglet has little impact on the flutter speed of the wing. Changing the twist of the wing is another option that modifies the aerodynamic loads on the wing. Twist morphing was one of the popular concepts considered over the recent decades, and several concepts have been introduced [4]. Several studies considered the effect of twist morphing on roll control [13], the minimization of induced drag [14], the aerodynamic performance [15], and the drag performance [16]. Farsadi et al. [17] considered the nonlinear aeroelasticity of linearly pre-twisted wings using thin-walled beam theory, and showed that the twisted wing can have higher flutter speed compared to the clean wing.

Recently, it has been proposed that making the wings curved can result in a reduction of drag and fuel burn [18]. Making the wings curved is an idea that is inspired from nature, and it was shown that a drooped wing shape could decrease the wing drag by up to 6%, and an inflected wing may result in a drag reduction of 4%. Although making aircraft wings with initial curvature can have some benefits on the aerodynamics, it could also change the structural dynamics of the wing significantly. The effect of initial curvature on the dynamics of curved

beams has been extensively addressed by many researchers [19]. Hodges [20] showed that initially curved isotropic beams introduce stretch-bending coupling in the beam. Chang and Hodges [21] determined the vibration characteristics of curved beams by using fully intrinsic equations. They highlighted that the behavior of the beam when it is curved under load is different from the beam with identical beam with initial curvature. Therefore, the curvature of the wing not only influences the aerodynamics of the wing, also affects the aeroelastic behavior of the wing. This has received little attention in the literature, and therefore here the effect of initial curvature on the aeroelastic stability of aircraft wings is studied.

In this study, the aeroelastic behavior of an aircraft wing with initial curvature is investigated, and the change in the flutter speed and frequency with respect to the out of plane curvature is determined. The aeroelastic problem is formulated by combining the geometrical exact fully intrinsic beam equations [22] with the unsteady Peters' aerodynamic loads [23]. The effect of initial curvature is considered through the capability of the beam formulation. Finally, the effect of initial curvature on the dynamics, flutter speed, and flutter frequency of a typical wing is discussed.

2 PROBLEM STATEMENT

An aircraft wing with initial curvature, as shown in Figure 1, is considered. It is assumed that the wing has a constant curvature over the span of the wing. Two cases are considered here for investigating the effect of curvature on the aeroelastic instability of the wing. In the first case, it is considered that the span length or the perimeter of the wing is constant, and when it is curved the projected area of the wing decreases. In the second case, the projected area of the wing is considered to be constant, and therefore the span length of wing is not fixed. The curvature radius is denoted here as R_r, and the arc angle of the curved beam is defined as

$$\alpha = Lk_2 \tag{1}$$

where L and k_2 are the span length and the initial curvature of the beam, respectively. The curved shapes of the wing for these two categories are shown in Figure 2. It is noted that in this study, it is assumed that all the structural properties of the wing remain intact when an additional curvature is added to the wing.

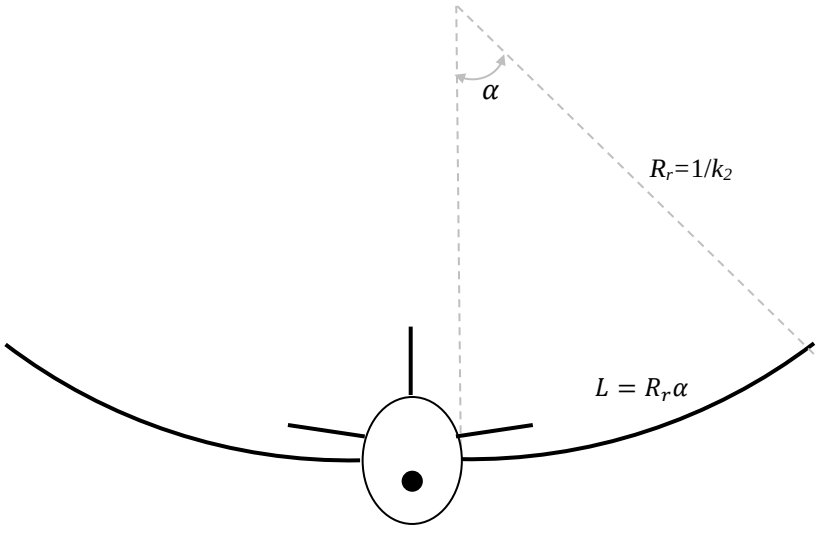

Figure 1: The schematic of the curved wing with constant initial curvature.

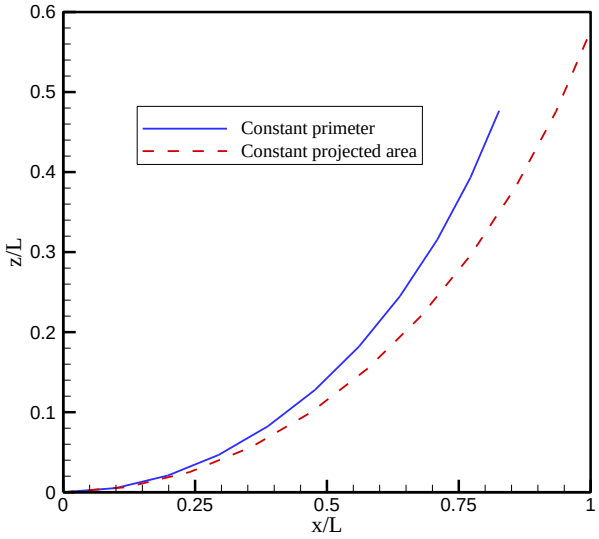

Figure 2: The curved shapes of the wing for constant perimeter and constant projected area assumptions for k_2=60°/m.

3 EQUATIONS OF MOTION

The curved wing of the aircraft is modeled by using the geometrically exact fully intrinsic beam equations [22]. This beam formulation has been used successfully recently for a range of different aerospace structure applications [24-30]. Thus:

$$
\begin{aligned}
&\partial F_1/\partial x_1 + K_2F_3 - K_3F_2 + f_{1_{aero}} = \partial P_1/\partial t + \Omega_2P_3 - \Omega_3P_2\\
&\partial F_2/\partial x_1 + K_3F_1 - K_1F_3 + f_{2_{aero}} = \partial P_2/\partial t + \Omega_3P_1 - \Omega_1P_3\\
&\partial F_3/\partial x_1 + K_1F_2 - K_3F_1 + f_{3_{aero}} = \partial P_3/\partial t + \Omega_1P_2 - \Omega_2P_1\\
&\partial M_1/\partial x_1 + K_2M_3 - K_3M_2 + 2\gamma_{12}F_3 - 2\gamma_{13}F_2 + m_{1_{aero}} = \partial H_1/\partial t + \Omega_2H_3 - \Omega_3H_2 + V_2P_3 - V_3P_2\\
&\partial M_2/\partial x_1 + K_3M_1 - K_1M_3 + 2\gamma_{13}F_1 - (1+\gamma_{11})F_3 + m_{2_{aero}} = \partial H_2/\partial t + \Omega_3H_1 - \Omega_1H_3 + V_3P_1 - V_1P_3\\
&\partial M_3/\partial x_1 + K_1M_2 - K_2M_1 + (1+\gamma_{11})F_2 - 2\gamma_{12}F_1 + m_{3_{aero}} = \partial H_3/\partial t + \Omega_1H_2 - \Omega_2H_1 + V_1P_2 - V_2P_1\\
&\partial V_1/\partial x_1 + K_2V_3 - K_3V_2 + 2\gamma_{12}\Omega_3 - 2\gamma_{13}\Omega_2 = \partial\gamma_{11}/\partial t\\
&\partial V_2/\partial x_1 + K_3V_1 - K_1V_3 - (1+\gamma_{11})\Omega_3 + 2\gamma_{13}\Omega_1 = 2\partial\gamma_{12}/\partial t\\
&\partial V_3/\partial x_1 + K_1V_2 - K_2V_1 + (1+\gamma_{11})\Omega_2 - 2\gamma_{12}\Omega_1 = 2\partial\gamma_{13}/\partial t\\
&\partial\Omega_1/\partial x_1 + K_2\Omega_3 - K_3\Omega_2 = \partial\kappa_1/\partial t\\
&\partial\Omega_2/\partial x_1 + K_3\Omega_1 - K_1\Omega_3 = \partial\kappa_2/\partial t\\
&\partial\Omega_3/\partial x_1 + K_1\Omega_2 - K_2\Omega_1 = \partial\kappa_3/\partial t
\end{aligned}
\tag{1}
$$

where F_i and M_i for i=1,2,3 are the sectional internal forces and moments, V_i and Ω_i are the linear and angular velocities, P_i and H_i are vectors containing the sectional linear and angular momenta, respectively. γ_{1i} and κ_{1i} are the generalized strains of the beam. The vector of final curvature and twist of the deformed beam is shown by K_i which can be described by

$$K_i = \kappa_i + k_i \tag{2}$$

where k_i denotes the initial curvature and twist values of the beam.
All variables that appeared in Eq (2) are described in the deformed coordinate reference system except the initial curvature and twist which are based on the undeformed reference frame. In

this study, it is assumed that the wing has an initial curvature and therefore k_i is not zero. The force and moment vectors are related to the generalized strain through the stiffness matrix as follows

$$\begin{bmatrix} F_1 \\ F_2 \\ F_3 \\ M_1 \\ M_2 \\ M_3 \end{bmatrix} = \begin{bmatrix} S_{11} & S_{12} & S_{13} & S_{14} & S_{15} & S_{16} \\ S_{12} & S_{22} & S_{23} & S_{24} & S_{25} & S_{26} \\ S_{13} & S_{23} & S_{33} & S_{34} & S_{35} & S_{36} \\ S_{14} & S_{24} & S_{34} & S_{44} & S_{45} & S_{46} \\ S_{15} & S_{25} & S_{35} & S_{45} & S_{55} & S_{56} \\ S_{16} & S_{26} & S_{36} & S_{46} & S_{56} & S_{66} \end{bmatrix} \begin{bmatrix} \gamma_{11} \\ 2\gamma_{12} \\ 2\gamma_{13} \\ \kappa_1 \\ \kappa_2 \\ \kappa_3 \end{bmatrix} \quad or \quad \begin{bmatrix} \boldsymbol{F} \\ \boldsymbol{M} \end{bmatrix} = [\boldsymbol{S}] \begin{bmatrix} \boldsymbol{\gamma} \\ \boldsymbol{\kappa} \end{bmatrix} \tag{3}$$

where ***S*** contains the stiffness components of the beam cross-section. Moreover, the linear and angular momenta can be calculated as follows

$$\begin{bmatrix} P_1 \\ P_2 \\ P_3 \\ H_1 \\ H_2 \\ H_3 \end{bmatrix} = \begin{bmatrix} \mu & 0 & 0 & 0 & \mu x_3 & -\mu x_2 \\ 0 & \mu & 0 & -\mu x_3 & 0 & 0 \\ 0 & 0 & \mu & \mu x_2 & 0 & 0 \\ 0 & -\mu x_3 & \mu x_2 & i_2 + i_3 & 0 & 0 \\ \mu x_3 & 0 & 0 & 0 & i_2 & i_{23} \\ -\mu x_2 & 0 & 0 & 0 & i_{23} & i_3 \end{bmatrix} \begin{bmatrix} V_1 \\ V_2 \\ V_3 \\ \Omega_1 \\ \Omega_2 \\ \Omega_3 \end{bmatrix} \tag{4}$$

where μ is the mass per unit length of the wing, $\mathbf{x}= [x_1, x_2, x_3]^{\mathrm{T}}$ is a vector containing the offsets between the mass centroid and the section reference line, and $\mathbf{i} = [i_1, i_2, i_3]^{\mathrm{T}}$ is the vector of mass moments of inertia.

The wing is subjected to incompressible unsteady aerodynamic loads simulated here by using the fully intrinsic representation of Peters' formulation ([23]) as follows:

$$\begin{aligned} f_{i_{aero}} &= C_a F_{i_a} && \text{for} \quad i = 1,2,3 \\ m_{i_{aero}} &= C_a M_{i_a} + C_a \tilde{y}_{ac} F_{i_a} && \text{for} \ i = 1,2,3 \end{aligned} \tag{5}$$

where C_a is the transformation matrix from the aerodynamic coordinate system to the beam reference coordinate system, the superscript ($\tilde{}$) is the tilde operator, which transforms a vector like **A** to its corresponding matrix as follows:

$$A = [a_1, a_2, a_3]^T, \qquad \tilde{A} = \begin{bmatrix} 0 & -a_3 & a_2 \\ a_3 & 0 & -a_1 \\ -a_2 & a_1 & 0 \end{bmatrix} \tag{6}$$

Moreover, F_{i_a}, M_{i_a} for i=1,2,3 are the aerodynamic forces and moments on the aerodynamic coordinate system that can be written as follows

$$\begin{aligned} F_{1_a} &= 0 \\ F_{2_a} &= \rho b \left(-C_{l_0} V_T V_{a_3} + C_{l_\alpha} \left(V_{a_3} + \lambda_0 \right)^2 - C_{d_0} V_T V_{a_2} \right) \\ F_{3_a} &= \rho b \left(C_{l_0} V_T V_{a_2} - C_{l_\alpha} \dot{V}_{a_3} b/2 - C_{l_\alpha} V_{a_2} \left(V_{a_3} + \lambda_0 - \Omega_{a_1} b/2 \right) - C_{d_0} V_T V_{a_3} \right) \\ M_{1_a} &= 2\rho b^2 \left(C_{m_0} V_T^2 - C_{m_\alpha} V_T V_{a_3} - C_{l_\alpha} V_{a_2} \Omega_{a_1} b/8 - C_{l_\alpha} \left(b^2/32 \dot{\Omega}_{a_1} - b/8 \dot{V}_{a_3} \right) \right) \\ M_{2_a} &= M_{3_a} = 0 \end{aligned} \tag{7}$$

where C_{l_0}, C_{l_α}, C_{d_0}, C_{m_0}, and C_{m_α} are the aerodynamic coefficients of the airfoil. The subscript $(\quad_a)$ refers to the aerodynamic coordinate system, and V_T is the total aerodynamic velocity that can be written as

$$V_T = \sqrt{V_{a_2}^2 + V_{a_3}^2} \tag{8}$$

Furthermore, λ_0 is the inflow value which is obtained based on the following relation [23]:

$$\begin{aligned} &[A]\{\dot{\lambda}\} + \left(\frac{V_T^n}{B^n}\right)\{\lambda\} = \left(-\dot{V}_{a_3} + \frac{b}{2}\dot{\Omega}_{a_3}\right)\{C\} \\ &\lambda_0 = \frac{1}{2}\{B\}^T\{\lambda\} \end{aligned} \tag{9}$$

where λ is a vector containing the inflow states and *A*, *B*, and *C* are constant matrices defined as

$$\begin{aligned} &[A] = [D + dB^T + Cd^T + \frac{1}{2}CB^T] \\ &B_n = (-1)^{n-1}\frac{(N+n-1)!}{(N-n-1)!}\frac{1}{(n!)^2} \qquad n \neq N \\ &B_n = (-1)^{n-1} \qquad n = N \\ &C_n = \frac{2}{n} \\ &d_n = \frac{1}{2} \qquad (n \neq 1) \\ &d_n = 0 \qquad (n = 1) \\ &D_{nm} = \frac{1}{2n} \qquad (n = m+1) \\ &D_{nm} = -\frac{1}{2n} \qquad (n = m-1) \\ &D_n m = 0 \qquad (n \neq m \mp 1) \end{aligned} \tag{10}$$

As the wing is completely fixed at the root and free at the tip, the following set of boundary conditions are applied to the equations of motion:

$$\begin{bmatrix} F_1(L,t) \\ F_2(L,t) \\ F_3(L,t) \end{bmatrix} = \begin{bmatrix} 0 \\ 0 \\ 0 \end{bmatrix}, \begin{bmatrix} M_1(L,t) \\ M_2(L,t) \\ M_3(L,t) \end{bmatrix} = \begin{bmatrix} 0 \\ 0 \\ 0 \end{bmatrix}, \begin{bmatrix} V_1(0,t) \\ V_2(0,t) \\ V_3(0,t) \end{bmatrix} = \begin{bmatrix} 0 \\ U_\infty \\ 0 \end{bmatrix}, \begin{bmatrix} \Omega_1(0,t) \\ \Omega_2(0,t) \\ \Omega_3(0,t) \end{bmatrix} = \begin{bmatrix} 0 \\ 0 \\ 0 \end{bmatrix} \tag{11}$$

where, U_∞ is the free steam velocity.
The governing aeroelastic equations of the wing are discretized by using a space-time discretization scheme [22]. By selecting the number of elements to 16, the results converged. Finally, to study the aeroelastic stability, first the steady state solution of the system is determined. Then, the eigenvalues of the linearized system about the steady-state condition are determined. By checking the resulting eigenvalues, the stability of the system can be obtained.

4 NUMERICAL RESULTS

To check the validity of the code, the nondimensional frequencies of a beam with initial curvature are determined and compared with those reported by [31], and presented in Table 1. In this case, the curvature angle is $\alpha = 180^o$, and the results shows a good agreement.

In the next step, the flutter speed of an aircraft wing is determined and compared with [32]. The wing resembles the Goland wing, and the wing properties are presented in Table 2. The flutter speed and flutter frequency of this wing are determined and compared with the results presented by [32] in Table 3. It is clear that the aeroelastic results by the present method are in a very good agreement with those of Rosa and Franciosi [30]. In the following section, the effect of the initial curvature on the flutter speed and frequency of the Goland wing is determined.

Table 1: The Comparison of the nondimensional frequencies of a curved cantilever beam

Mode No.	Present	Rosa and Franciosi [31]
1st	0.43541	0.435
2nd	1.3781	1.375
3rd	4.7311	4.71
4th	10.604	10.52

Table 2: Goland wing structural and aerodynamic properties

Parameter	Definition	Value
L	Wing half span	6.1 m
c	Wing root chord	1.83 m
GJ	Torsional Stiffness	0.99×10^6 N.m^2
EI_2	Bending Stiffness	9.77×10^6 N.m^2
μ	Mass per unit length	35.7 kg/m
i_3	Mass moment of inertia	8.64 kg.m
$x_{e.a.}$	Elastic axis offset from L.E.	33% chord
$x_{c.g.}$	Centre of gravity offset from L.E.	43% chord
y_{ac}	Aerodynamic center offset from L.E.	25% chord
C_{l_α}	Lift curve slope	2π
$\lambda = EI_2/GJ$	Stiffness ratio	7.5-12.5

Table 3: Comparison of the flutter speed and flutter frequency of Goland wing

	Present	Patil et al. [32]
Flutter speed (m/s)	135.6	136
Flutter frequency (rad/s)	70.23	70.2

When the initial curvature is added to the wing, the aeroelastic properties of the wing changes, and therefore it is important to check the impact on the onset of instability. As mentioned earlier,

the wing has an initial out of plane curvature, k_2, which is assumed to be constant along the span of the wing. The deformed shape of the wing for various curvature angles is shown in Figure 3. In this case, it is assumed that span or the perimeter of the wing is constant.

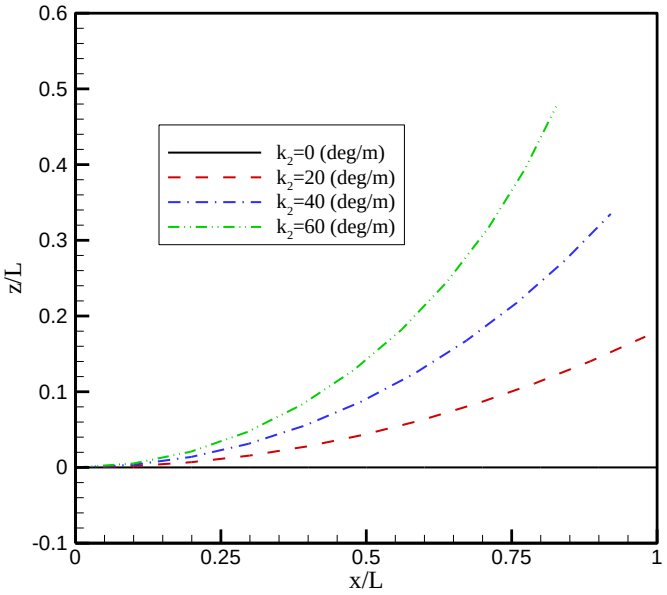

Figure 3: The deformed shape of the wing for the constant perimeter case.

First, the effect of the initial curvature on the three first natural frequencies of the wing is determined and shown in Figure 4. By increasing the initial curvature of the wing, the two first frequencies approach each other until a certain value of curvature, but after that they veer away each other. In this case, the veering occurs when the initial curvature is about $k_2 = 55^o/m$.

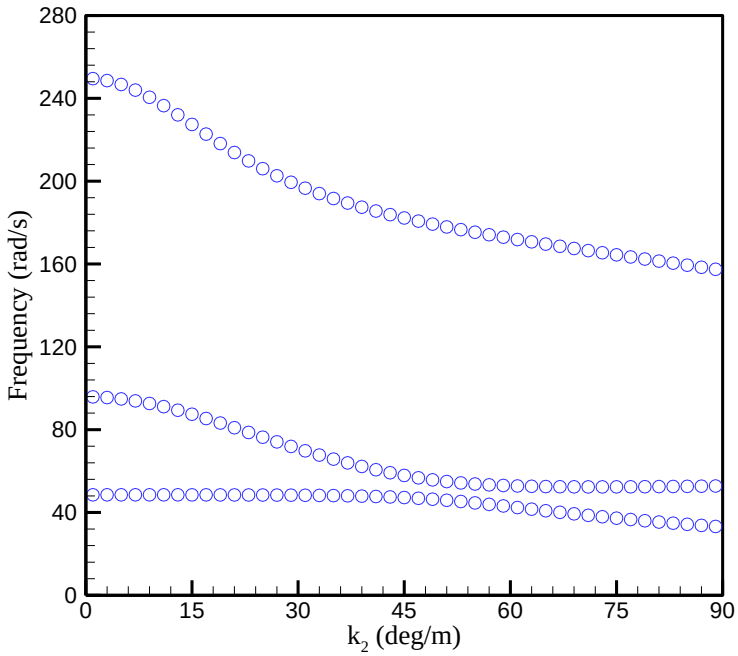

Figure 4: The natural frequencies of the wing for different values of out of plane curvature.

Next, the effect of initial curvature on the flutter speed and frequency of the wing for the case of constant perimeter is determined. Figure 5 shows the change in flutter speed of the wing for various initial out of plane curvature angles. When the initial curvature is added to the wing, at

first the flutter speed decreases until about $k_2 = 45^o/m$, mostly due to the initial coalescence of the first and second modes, as shown in Figure 4. Then, the flutter speed increases gradually until about $k_2 = 67^o/m$ where the interaction between the first and second modes is still the main cause of flutter, but these modes then veer away each other. Then a sudden increase is observed in flutter speed which is mainly due to the flutter mechanism changing. Again, after this point the flutter speed decreases. Furthermore, as shown in Figure 6, the flutter frequency of the wing also decreases gradually until $k_2 = 67^o/m$ where there is a jump in the flutter frequency, and then again it reduces. The main reason for this sudden jump in the flutter speed and flutter frequency is the change in the flutter modes as described below.

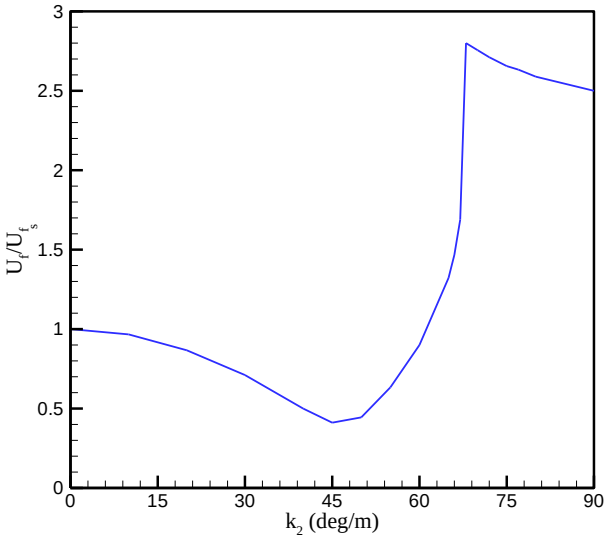

Figure 5: Flutter speed versus out of plane curvature for the constant perimeter case,

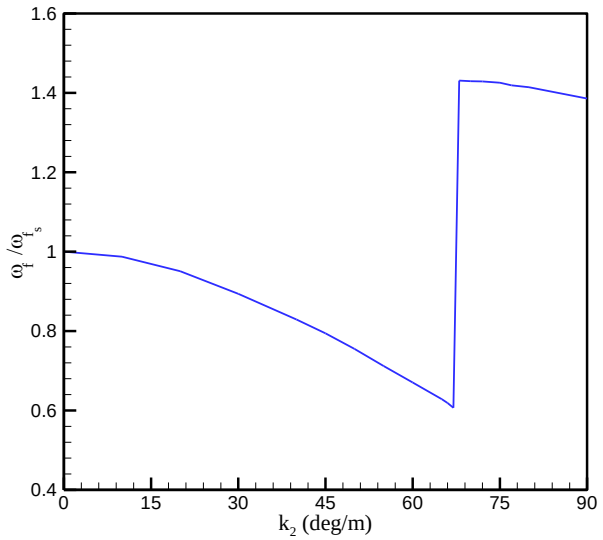

Figure 6: Flutter frequency versus out of plane curvature for the constant perimeter case.

For the domain of initial curvature of $k_2 < 67^o$, as shown in Figure 7, the flutter is the result of coupling between the first and second modes. Also, it must be noted that in this region, by increasing the aircraft speed, initially the first and second modes are coupled together, but after a certain value above the flutter speed, the first and third modes are coupled together. Moreover, for the domain of $k_2 \geq 67^o/m$, as shown in Figure 8, at the beginning the two first modes approach together but then veer away from each other. Then, the first and third modes are

coupled together which results in higher flutter speeds. This completely clarifies the reason for the sudden jump shown in the flutter speed and flutter frequency.

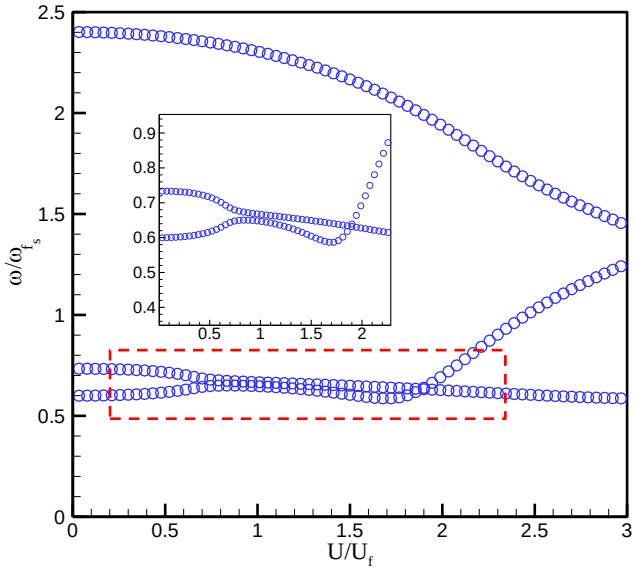

Figure 7: Aeroelastic frequencies versus velocity for k_2=60 deg/m,

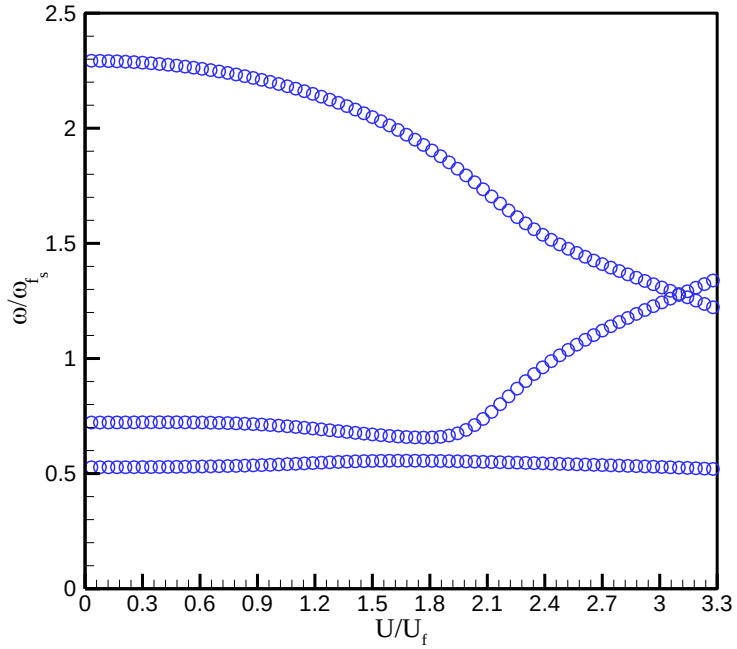

Figure 8: Aeroelastic frequencies versus velocity for k_2=75 deg/m.

Figures 9 and 10 show the variation of flutter speed and flutter frequency of the wing with respect to the initial curvature for different stiffness ratios ($\lambda = EI_2/GJ$). The stiffness ratio completely affects the flutter speed of the wing, but the trend of the change is different for various initial curvature angles. When the stiffness ratio decreases, the point at which the flutter speed trend changes moves forward toward higher values of curvature angle. Moreover, three regions are clear in Figure 9 where the stiffness ratio works differently. In the first and third regions the flutter speed decreases by increasing the initial curvature, and when λ decreases, the flutter speed increases. But the situation is completely different in the middle region the flutter speed increases by increasing the curvature angle. In this region, when the stiffness ratio raises, the flutter speed also increases. This highlights the importance of the combination of the

stiffness ratio and initial curvature on the flutter speed. Moreover, the stiffness ratio also affects the flutter frequency as shown in Figure 10. For all initial curvature values, by increasing the stiffness ratio, the flutter frequency also increases, but the rate of increase is not constant.

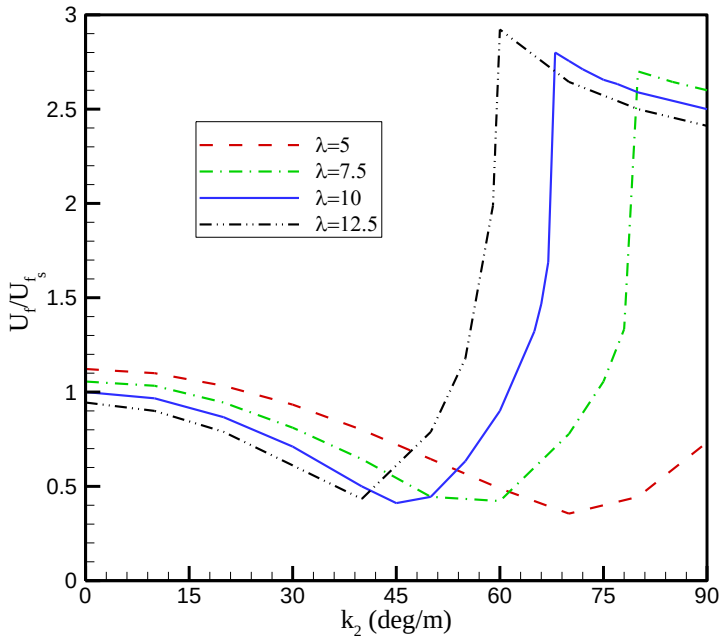

Figure 9: The effect of λ on the flutter speed for various initial curvatures,

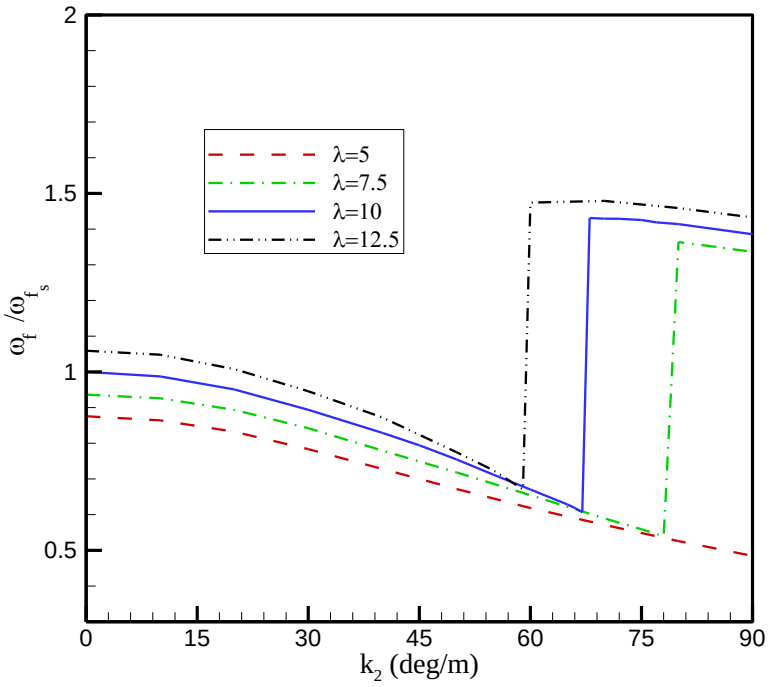

Figure 10: The effect of λ on the flutter frequency for various initial curvatures.

Finally, Figures 11 and 12 shows the flutter speed and flutter frequency of the wing for the two cases of constant perimeter and constant projected area. In this case, the stiffness ratio is considered to be λ=10. For lower values of initial curvature, there is no significant difference between the flutter speed of these two cases, as shown in Figure 11. But for higher values of

curvature angles, the difference tends to get larger. This pattern is also observed in Figure 12 for the flutter frequency. Therefore, this mainly highlights that in terms of extending the stability region, the case of constant perimeter works better than the case of constant projected area.

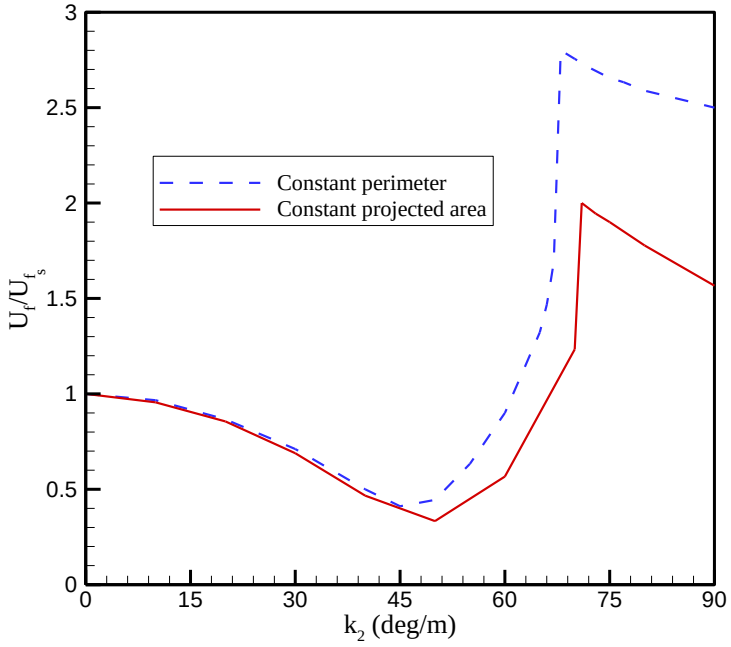

Figure 11: Flutter speed for the constant perimeter case versus constant projected area for various initial curvatures,

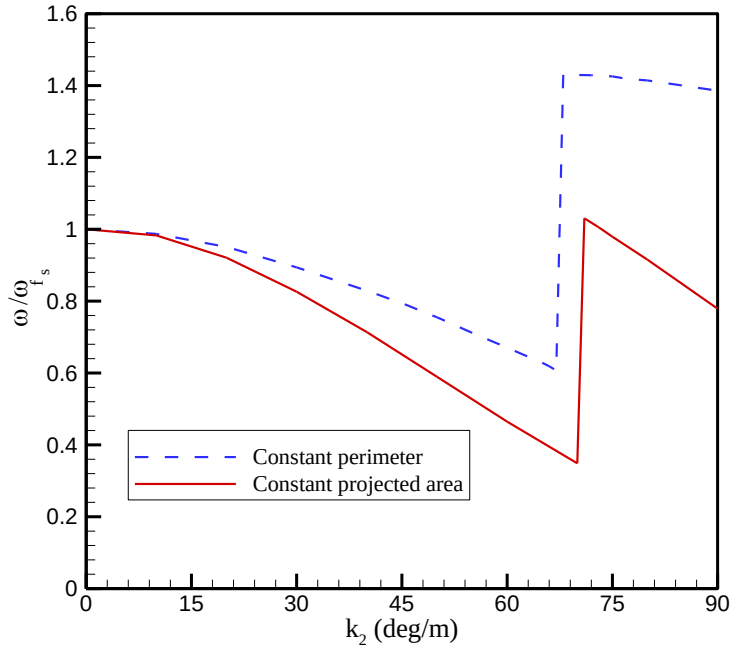

Figure 12: Flutter frequency for the constant perimeter case versus constant projected area for various initial curvatures.

5 CONCLUSION

In this paper, the aeroelastic stability of a curved aircraft wing is investigated. The wing is considered to have an out of plane curvature which might have advantages in reducing the drag. The wing is modeled by using the geometrically exact fully intrinsic beam equations and the curvature is considered by adding the initial curvature to the beam formulations. The aerodynamic loads applied on the wing are simulated using an incompressible unsteady aerodynamic model. The resulting aeroelastic equations are discretized using a time-space scheme, and the stability of the system is determined through an eigenvalue analysis. It has been shown that when the curvature is added to the wing, the frequencies of the wing changes. Furthermore, when the initial curvature is introduced to the wing, the flutter speed and flutter frequency of the wing changes completely. Moreover, a sudden jump in the flutter speed and frequency was seen in a certain curvature angle which is mostly due to the change in the modes contributing to the flutter. Finally, the effects of stiffness ratio combined with the initial curvature of the wing on the flutter speed and frequency of the wing have been presented.

6 REFERENCES

1. Bairstow, L., and Fage, A. "Oscillation of the taiplane and body of an aeroplane in flight," *A.R.C. R. & M. 276, part 2*, 1916.
2. Goland, M. "The flutter of a uniform cantilever wing," *Journal of Applied Mechanics* Vol. 12, No. 4, 1945, pp. A197-A208.
3. Goland, M., and Luke, Y. L. "The flutter of a uniform wing with tip weights," *Journal of Applied Mechanics* Vol. 15, 1948, pp. 13-20.
4. Li, D., Zhao, S., Da Ronch, A., Xiang, J., Drofelnik, J., Li, Y., Zhang, L., Wu, Y., Kintscher, M., Monner, H. P., Rudenko, A., Guo, S., Yin, W., Kirn, J., Storm, S., and Breuker, R. D. "A review of modelling and analysis of morphing wings," *Progress in Aerospace Sciences* Vol. 100, 2018, pp. 46-62.
5. Barbarino, S., Bilgen, O., Ajaj, R. M., Friswell, M. I., and Inman, D. J. "A Review of Morphing Aircraft," *Journal of Intelligent Material Systems and Structures* Vol. 22, No. 9, 2011, pp. 823-877.
6. Lottati, I. "Aeroelastic stability characteristics of a composite swept wing with tip weights for an unrestrained vehicle," *Journal of Aircraft* Vol. 24, No. 11, 1987, pp. 793-802.
7. Gern, F. H., and Librescu, L. "Static and dynamic aeroelasticity of advanced aircraft wings carrying external stores," *AIAA Journal* Vol. 36, No. 7, 1998, pp. 1121-1129.
8. Mazidi, A., and Fazelzadeh, S. A. "Flutter of a Swept Aircraft Wing with a Powered Engine," *Journal of Aerospace Engineering* Vol. 23, No. 4, 2010, pp. 243-250.
9. Goetz, R. C., and Doggett, R. V. "Some effects of tip fins on wing flutter characteristics," *NASA TN D-7702*, 1974.
10. Doggett, R. V., and Farmer, M. G. "Preliminary study of effects of winglets on wing flutter," *NASA TM X-3433*, 1976.
11. Cui, P., and Han, J. "Prediction of flutter characteristics for a transport wing with wingtip devices," *Aerospace Science and Technology* Vol. 23, No. 1, 2012, pp. 461-468.
12. Lv, B., Lu, Z., Guo, T., Tang, D., Yu, L., and Guo, H. "Investigation of winglet on the transonic flutter characteristics for a wind tunnel test model CHNT-1," *Aerospace Science and Technology* Vol. 86, 2019, pp. 430-437.
13. Pecora, R., Amoroso, F., and Lecce, L. "Effectiveness of Wing Twist Morphing in Roll Control," *Journal of Aircraft* Vol. 49, No. 6, 2012, pp. 1666-1674.
14. Hunsaker, D. F., Montgomery, Z. S., and Joo, J. J. "Lifting-Line analysis of wing twist to minimize induced drag during pre roling moion," *AIAA Scitech 2019 Forum*, 2019.
15. Rodrigue, H., Cho, S., Han, M.-W., Bhandari, B., Shim, J.-E., and Ahn, S.-H. "Effect of twist morphing wing segment on aerodynamic performance of UAV," *Journal of Mechanical Science and Technology* Vol. 30, No. 1, 2016, pp. 229-236.

16. Ismail, N. I., Zulkifli, A. H., Talib, R. J., Zaini, H., Yusoff, H., Sahari, B. B., Qin, Q., and Das, R. "Drag performance of twist morphing MAV wing," *MATEC Web of Conferences 82, 01004*, 2016.
17. Farsadi, T., Rahmanian, M., and Kayran, A. "Geometrically nonlinear aeroelastic behavior of pretwisted composite wings modeled as thin walled beams," *Journal of Fluids and Structures* Vol. 83, 2018, pp. 259-292.
18. Nguyen, N., and Urnes, J. "Aeroelastic Modeling of Elastically Shaped Aircraft Concept via Wing Shaping Control for Drag Reduction," *AIAA Atmospheric Flight Mechanics Conference*.
19. Chidamparam, P., and Leissa, A. W. "Vibrations of Planar Curved Beams, Rings, and Arches," *Applied Mechanics Reviews* Vol. 46, No. 9, 1993, pp. 467-483.
20. Hodges, D. H. "Non-linear inplane deformation and buckling of rings and high arches," *International Journal of Non-Linear Mechanics* Vol. 34, No. 4, 1999, pp. 723-737.
21. Chang, C. S., and Hodges, D. H. "Vibration characteristics of curved beams," *Journal of Mechanics of Materials and Structures* Vol. 4, No. 4, 2009, pp. 675-692.
22. Hodges, D. H. "Geometrically Exact, Intrinsic Theory for Dynamics of Curved and Twisted Anisotropic Beams," *AIAA Journal* Vol. 41, No. 6, 2003, pp. 1131-1137.
23. Peters, D. A., Karunamoorthy, S., and Cao, W.-M. "Finite state induced flow models. I - Two-dimensional thin airfoil," *Journal of Aircraft* Vol. 32, No. 2, 1995, pp. 313-322.
24. Amoozgar, M. R., and Shahverdi, H. "Aeroelastic Stability Analysis of Curved Composite Blades in Hover Using Fully Intrinsic Equations," *International Journal of Aeronautical and Space Sciences*, 2019.
25. Amoozgar, M. R., Shaw, A. D., Zhang, J., and Friswell, M. I. "Composite Blade Twist Modification by Using a Moving Mass and Stiffness Tailoring," *AIAA Journal*, 2018, pp. Accepted, DOI: 10.2514/1.J057591.
26. Amoozgar, M. R., Shaw, A. D., Zhang, J., and Friswell, M. I. "The effect of a movable mass on the aeroelastic stability of composite hingeless rotor blades in hover," *Journal of Fluids and Structures* Vol. 87, 2019, pp. 124-136.
27. Chang, C.-S., and Hodges, D. H. "Parametric Studies on Ground Vibration Test Modeling for Highly Flexible Aircraft," *Journal of Aircraft* Vol. 44, No. 6, 2007, pp. 2049-2059.
28. Fulton, M. V., and Hodges, D. H. "Aeroelastic stability of composite hingeless rotor blades in hover—Part II: Results," *Mathematical and Computer Modelling* Vol. 18, No. 3, 1993, pp. 19-35.
29. Mardanpour, P., Hodges, D. H., Neuhart, R., and Graybeal, N. "Engine Placement Effect on Nonlinear Trim and Stability of Flying Wing Aircraft," *Journal of Aircraft* Vol. 50, No. 6, 2013, pp. 1716-1725.
30. Mardanpour, P., Izadpanahi, E., Rastkar, S., Fazelzadeh, S. A., and Hodges, D. H. "Geometrically Exact, Fully Intrinsic Analysis of Pre-Twisted Beams Under Distributed Follower Forces," *AIAA Journal* Vol. 56, No. 2, 2017, pp. 836-848.
31. De Rosa, M. A., and Franciosi, C. "Exact and approximate dynamic analysis of circular arches using DQM," *International Journal of Solids and Structures* Vol. 37, No. 8, 2000, pp. 1103-1117.
32. Patil, M. J., Hodges, D. H., and Cesnik, C. E. S. "Nonlinear aeroelastic analysis of aircraft with high-aspect-ratio wings," *39th AIAA/ASME/ASCE/AHS/ASC Structures, Structural Dynamics, and Materials Conference and Exhibit*. American Institute of Aeronautics and Astronautics, 1998.